Published online 23 January 2015 *Nucleic Acids Research, 2015, Vol. 43, No. 3* ***1759–1769***
doi: 10.1093/nar/gkv006

A basal level of DNA damage and telomere deprotection increases the sensitivity of cancer cells to G-quadruplex interactive compounds

Erica Salvati[1,†], Angela Rizzo[1,†], Sara Iachettini[1], Pasquale Zizza[1], Chiara Cingolani[1], Carmen D'Angelo[1], Manuela Porru[1], Chiara Mondello[2], Aurora Aiello[3,4], Antonella Farsetti[3,4], Eric Gilson[5,6], Carlo Leonetti[1] and Annamaria Biroccio[1,*]

[1]Experimental Chemotherapy Laboratory, Regina Elena National Cancer Institute, Rome, Italy, [2]Istituto di Genetica Molecolare, National Research Council (CNR), Pavia, Italy, [3]Institute of Cell Biology and Neurobiology (IBCN), CNR Rome, Italy, [4]Department of Experimental Oncology, Regina Elena National Cancer Institute, Rome, Italy, [5]Institute for Research on Cancer and Aging, Nice (IRCAN), CNRS UMR7284/INSERM U1081, University of Nice, Nice, France and [6]Department of Medical Genetics, Archet 2 Hospital, CHU of Nice, Nice, France

Received August 12, 2014; Revised January 05, 2015; Accepted January 06, 2015

ABSTRACT

Here, with the aim of obtaining insight into the intriguing selectivity of G-quadruplex (G4) ligands toward cancer compared to normal cells, a genetically controlled system of progressive transformation in human BJ fibroblasts was analyzed. Among the different comparative evaluations, we found a progressive increase of DNA damage response (DDR) markers throughout the genome from normal toward immortalized and transformed cells. More interestingly, sensitivity to G4 ligands strongly correlated with the presence of a basal level of DNA damage, including at the telomeres, where the chromosome ends were exposed to the DDR without concurrent induction of DNA repair activity, as revealed by the lack of 53BP1 recruitment and telomere aberrations. The link between telomere uncapping and the response to G4 stabilization was directly assessed by showing that a partial TRF2 depletion, causing a basal level of telomere localized DDR, rendered telomerized fibroblasts prone to G4-induced telomere damage and anti-proliferative defects. Taken together these data strongly indicate that the presence of a basal level of telomere-associated DDR is a determinant of susceptibility to G4 stabilization.

INTRODUCTION

Telomeres are the structures at the end of eukaryotic linear chromosomes. Human telomeres consist of double-stranded tandem repeats of the hexanucleotide sequence TTAGGG, except for a terminal 3′ G-rich overhang. Telomeres can form a loop structure (t-loop), with the 3′ G-rich strand invading the duplex telomeric tract (1), or can fold into a four-stranded DNA structure, termed G-quadruplex (G4) (2). To ensure telomeric function, this DNA structure is bound by various telomere-associated proteins: a core complex of six telomere-specific proteins (shelterin) and a growing number of accessory proteins that assist with proper chromosome end protection, telomere length regulation and telomere processing (3,4).

Telomeres serve two main purposes: they act as sequence buffer to counteract replication-associated shortening and they protect the ends of chromosomes from degradation and damage (5). Critically short or unprotected telomeres, obtained by deleting shelterin components (the best examples are TRF2 and POT1), result in acute phenotypes where the chromosome ends are recognized as double-strand break, eliciting either an ATM- or ATR-dependent DNA damage response (DDR), and are subjected to homologous recombination or fusion via non-homologous or alternative end-joining (6–9). Deprotected chromosome ends subjected to a DDR are cytologically visible as colocalizations between telomeric proteins (e.g. TRF1) or DNA and DDR markers, such as the phosphorylation of histone H2AX (γH2AX) within the telomeric and sub-telomeric chromatin and association of 53BP1 (53-binding protein 1) with the chromosome ends (10–12), forming the so-called Telomere-Dysfunction Induced Foci (10). Similar foci occur in smaller number at replicative senescence and there is evidence that these telomeric DDR signals are responsible for initiating p53-dependent senescence (13).

*To whom correspondence should be addressed. Tel: +39 6 52662569; Fax: +39 6 52662592; Email: biroccio@ifo.it
†These authors contributed equally to the paper as first authors.

An emerging model suggests that spontaneous telomere deprotection during aging progresses through three distinct protective states that regulate cellular consequences (14). In this model, telomere erosion controls proliferative boundaries by changing telomere structure from a 'closed state', that protects chromosome ends against DDR, into two distinct states of telomere deprotection: (i) the 'intermediate state', where telomeres induce DDR but bind sufficient shelterin to inhibit end-to-end fusion; (ii) the 'uncapped state', that is both DDR+ and fusogenic, resulting from insufficient TRF2 to inhibit end joining. Quantitative analysis indicates that five or more intermediate-state telomeres are sufficient to induce senescence, and more deprotected telomeres can accrue in p53 incompetent cells without affecting growth (15), in agreement with recent results demonstrating that telomeric DNA damage is irreparable and causes persistent DDR activation (16).

A wealth of published works revealed that uncapped telomeres can also be obtained by pharmacological G4 stabilization (17). Over the past decade, many chemical classes of G4 ligands have been described for their ability to target and damage telomeres, preferentially affecting transformed and tumor cells (18). Several of them reduce the growth of various cancer cell lines and some of them exhibit antitumor activity in mice bearing various human tumour xenografts, including some inherently resistant to chemotherapy (19). The effect of G4 ligands both as a single agent and, more interestingly, in combined therapy with cytotoxic agents widely used in cancer treatment, such as camptothecins, suggests that this class of compounds could be employed as very promising anticancer agents (20,21). A consistent mechanism of action is now emerging for G4 ligands: in addition to their telomerase inhibitory properties, these agents can exert an anticancer effect by telomeric chromatin alteration leading to POT1 and TRF2 dissociation with the consequent activation of ATR-/ATM-dependent damage pathway at the telomeres (21–23). However, the molecular mechanism of this new class of potential antineoplastic agents has not been fully understood. Here, we found that the presence of a basal degree of uncapped telomeres, characterizing tumor lines, can make cells susceptible to G4 stabilization, identifying one of the mechanism(s) responsible for the selectivity of G4 ligands toward transformed cells.

MATERIALS AND METHODS

Cells, culture condition and transfection

Human BJ, primary melanocytes, human epthelial kidney (HEK) and prostate epithelial (PrEC) cells were purchased by the ATCC repository and maintained according to the manufacturer's instructions. To obtain the BJ-hTERT cell line, primary BJ were infected with the hTERT carrying retrovirus (Addgene plasmid #1773; (24)). Early, Mid and Late cen 3 tel fibroblasts were obtained and maintained as described (25). BJ-EHLT, BJ-EHLT/RasV12 fibroblasts, M14 melanoma and PC3 prostate cancer cell lines were obtained and maintained as described (23,26–27). HEK+SV40LT cells were a generous gift of Dr. Silvia Bacchetti (28).

GFP, p53 and pRb interfered BJ-hTERT cells were obtained by infection with amphotrophic retroviruses generated by transient transfection of retroviral vectors expressing short hairpin for GFP, p53 (pBabe-puro-shGFP and pBabe-puro-shp53 are a kind gift of Dr. Grandori (29)), and pRb (Addgene plasmid 10670; (30)) into Phoenix amphotropic packaging cells with Lipofectamine 2000 (Invitrogen Carlsbad, CA, USA) according to the manufacturer's instruction. For transient RNA interference experiments, siTRF2 and siGFP were purchased from Dharmacon Inc. (Chicago, USA) and transfected in BJ h-TERT with Lipofectamine 2000 according to the manufacturer's instruction.

In vitro treatment, proliferation and viability assays

The G4 ligand RHPS4 was synthesized and used as described previously (31,32). Note that 5×10^4 cells were seeded in 60-mm Petri plates and 24 h after plating, the freshly dissolved drugs were added to the culture medium. Cell counts and viability (trypan blue dye exclusion) were determined daily, from day 1 to day 12 of culture.

Western blotting (WB)

Western blot and detection were performed as previously reported (33). For WB application, the following antidodies were used: mAb anti-β-actin (Sigma Chemicals, Milano, Italy), mAb anti-p53 DO-1, pAb anti-Thr68 Chk2 (Cell Signaling, Beverly, MA, USA); mAb anti-TRF2 (Imgenex, San Diego, CA, USA); mAb anti-pRB (BD Pharmingen, Franklin Lakes, NJ, USA).

Immunofluorescence (IF) and fluorescence *in situ* hybridization (FISH)

For interphase nuclei telomere-induced foci (TIFs) analysis, cells were fixed in 2% formaldehyde and permeabilized in 0.25% Triton X100 in phosphate buffered saline (PBS) for 5 min at room temperature (RT). Then cells were incubated with primary antibodies for 2 h at RT, then washed in PBS and incubated with the following secondary antibodies: tetramethylrhodamine (TRITC)-conjugated Goat anti-Rabbit, fluorescein isothiocyanate (FITC)-conjugated Goat anti-Mouse (Jackson ImmunoResearch, West Grove, PA, USA). Nuclei were counterstained with 4',6-diamidino-2-phenylindole, Sigma (DAPI).

For metaphase TIFs analysis cells were processed as described in (34). Briefly, cells were blocked with demecolcine solution (20 ng/ml) for 1 h and then harvested and resuspended in hypotonic buffer. Then cells were cytospun onto glass slides and then fixed and processed for immunolabeling with γH2AX primary antibody, and successively with a FITC-conjugated Goat anti-Mouse secondary antibody. Hybridization with TelG-Cy3 probe (Panagene, Daejeon, Korea) was performed as described (35). For the cytogenetic evaluation of telomere aberrances, cells blocked in demecolcine as above reported were collected and washed in hypotonic buffer and processed as described (36). Fluorescence signals were recorded by using a Leica DMIRE2 microscope equipped with a Leica DFC 350FX camera and elaborated by a Leica FW4000 deconvolution software (Leica, Solms, Germany). For Q-FISH analysis the acquired fluorescence signals were quantified by the TFL-Telo software.

For IF application, the following antibodies were used: Mouse mAb anti-γH2AX (Millipore, Billerica, MA, USA); Mouse mAb (Abcam Ltd., Cambridge, UK) and Rabbit pAb anti-TRF1 (Santa Cruz Biotechnologies, Santa Cruz, CA, USA) Rabbit pAb anti-53BP1 (Novus Biological Inc., Littleton, CO, USA); Mouse mAb anti-γH2AX (Millipore).

Chromatin immunoprecipitaion (ChIP) assay

ChIP assay was performed as previously described (37). The following antibodies were used: pAb anti-TRF1 (Santa Cruz Biotechnology, Santa Cruz, CA, USA); mAb anti-TRF2 (Imgenex, San Diego, CA, USA); pAb anti-γH2AX (ab2893, Abcam). mAb anti-β-actin (Sigma) was used as negative control of the ChIP assay.

Statistical analysis

The experiments have been repeated from three to five times and the results obtained are presented as means ± SD. Significant changes were assessed by using Student's *t*-test two tails for unpaired data, and *P*-values <0.05 were considered significant.

RESULTS

Transformation makes cells sensitive to G-quadruplex-stabilizing agents

Several small molecules interacting with G4s, which have been described as telomere-targeting agents, display an intriguing selectivity toward transformed and tumor cells (19). In this context, by using a genetically controlled cell system of human primary (BJ), immortalized (BJ-hTERT) and SV40LT transformed (BJ-EHLT) foreskin fibroblasts, we demonstrated that normal and telomerized cells were resistant to different chemically unrelated G4 ligands, when using a drug dose able to kill transformed cells (21,23; Figure 1A and Supplementary Figure S1). This phenomenon is exacerbated when BJ-EHLT cells were transfected with Ras/V12 oncogene (BJ-EHLT/Ras), showing that the acquisition of a tumorigenic phenotype makes cells more sensitive to telomere damaging agents (Figure 1A and Supplementary Figure S1). These results were confirmed by using a model of stepwise neoplastic transformation of h-TERT immortalized fibroblasts (25,38). In this case, Early- as well as Mid-passage cells, which did not show transformed morphology, were almost resistant to the G4-stabilizing agent RHPS4 while Late-passage fibroblasts, which underwent spontaneous transformation *in vitro*, developing a pre-neoplastic (Late I) or neoplastic (Late III) phenotype (25,38), were sensitive to the G4 ligand (Figure 1B). In order to rule out a fibroblast-specific effect regarding G4 ligand sensitivity, we evaluated the response to RHPS4 on human cells of different histotype, by comparing primary melanocytes with the M14 melanoma line, HEK epithelial kidney cells with their SV40-transformed counterpart, and PrEC prostate cells with the PC3 tumor cells. In all cases, RHPS4 triggered inhibition of cell proliferation in the transformed or tumor counterpart, without affecting the viability of the corresponding normal cells (Figure 1C and D). We conclude that transformation itself confers sensitivity toward G4 ligands.

It is worth mentioning that a progressive decrease of cell proliferation (Figure 2A), accompanied by a massive induction of DNA damage (Figure 2B), including at telomeres (Figure 2C–G), was observed in normal cells at higher doses of drug exposure (2 and 5 μM), indicating that RHPS4 displays a narrow window for selectivity between dividing normal and tumor cells. The fact that roughly four times more of RHPS4 is required to target telomeres and to decrease cell viability is an important feature in the light of a future clinical application of this new class of potential anti-tumor agents.

To understand why tumor cells are particularly sensitive to G4 stabilization, we first excluded an eventual different drug uptake between normal and transformed cells (Supplementary Figure S2). Then we asked whether mechanisms causing the slow growth of normal versus the rapid proliferation of tumor cells may be involved. The fact of growing normal BJ-hTERT fibroblasts in 20% fetal calf serum (FCS), which increased by 2-fold the percentage of S-phase cells, as compared to cells grown in 10% FCS, did not render them sensitive to RHPS4 (Supplementary Figure S3A–C). The resistance to RHPS4 of highly proliferating human peripheral blood lymphocytes are in agreement with these results (Supplementary Figure S3D and E). Conversely, BJ-EHLT cells growing in 5% FCS, reducing the number of dividing cells, did not decrease their sensitivity to the drug treatment (Supplementary Figure S3A–C). Moreover, to reveal even a transient response to G4 stabilization, BJ-hTERT cells were synchronized at the G1/S boundary with the thymidine block, and the kinetics of a DDR activation was monitored after release. As reported in Supplementary Figure S4, we did not detect any activation of damage response at all the times analyzed, even in S phase cells, corresponding to active telomere replication (6). Overall, these results failed to reveal a significant contribution of cell proliferation to the G4 ligand sensitivity.

A basal level of telomere uncapping is associated with G4 ligand sensitivity.

Then, we investigated whether the differential sensitivity to G4 ligand between normal and transformed cells was due to differences in the structure of their telomeres. Consistent with the reactivation of telomerase activity, the telomere length and the amount of telomere bound shelterin proteins were increased in BJ-hTERT (resistant) as well as in BJ-EHLT and BJ-EHLT/Ras (sensitive) fibroblasts (Supplementary Figure S5A, C and D), while no difference in the length of 3′-overhang was detected in the various cell lines (Supplementary Figure S5B). Moreover, qFISH analysis did not show more critically short telomeres in BJ-EHLT and BJ-EHLT/Ras cells then in normal and BJ-hTERT fibroblasts (Supplementary Figure S5E). Thus, differences in RHPS4 sensitivity cannot be merely explained by telomere length changes.

Remarkably, the high level of sensitivity of BJ-EHLT and BJ-EHLT/Ras cells as compared to BJ and BJ-hTERT cells was associated with an increased basal level of DDR, both globally, as scored in interphase cells by the number

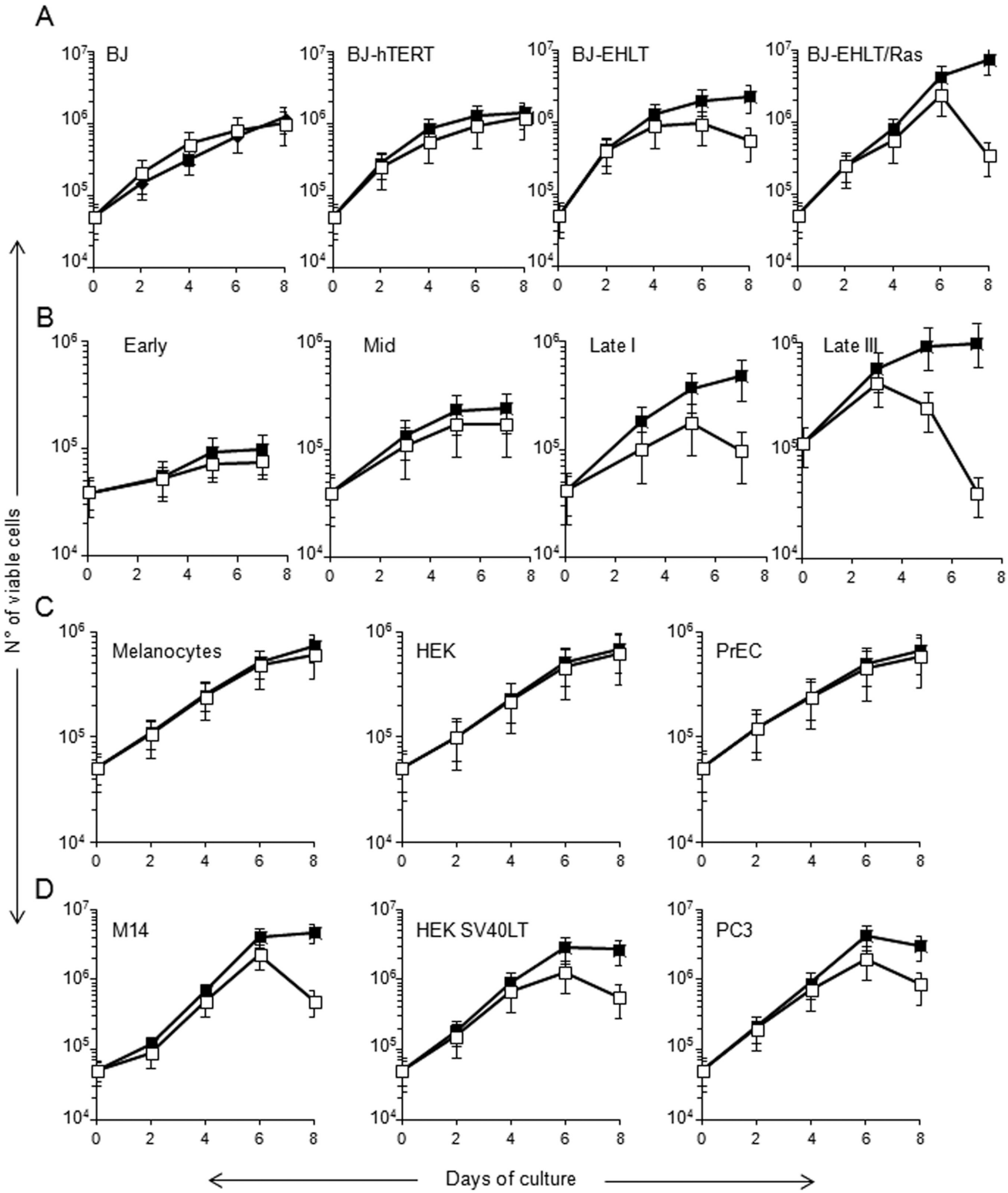

Figure 1. Transformation makes cells sensitive to RHPS4. The following lines were treated with 0.5 μM RHPS4: human primary (BJ), immortalized (BJ-hTERT), SV40LT transformed (BJ-EHLT) and transfected with RasV12 oncogene (BJ-EHLT/Ras) foreskin fibroblasts (**A**); cen 3 tel human fibroblasts immortalized with hTERT at early and mid *in vitro* passages (Early and Mid) and after neoplastic transformation (Late phase I and phase III tumorigenic cells) (**B**); primary (**C**) and tumor cells (**D**) of the same histological origin (melanoma-derived cell line M14 and primary melanocytes; SV40 transformed with parental HEK cells; Prostate Cancer PC3 cell line with prostate epithelial cells -PrEC-). At the indicated times, cells were counted and the viability determined. The data represent the number of untreated (filled squares) and RHPS4-treated cells (open squares) during the growth in culture. The mean of three independent experiments with comparable results is shown. Error bars indicate SD.

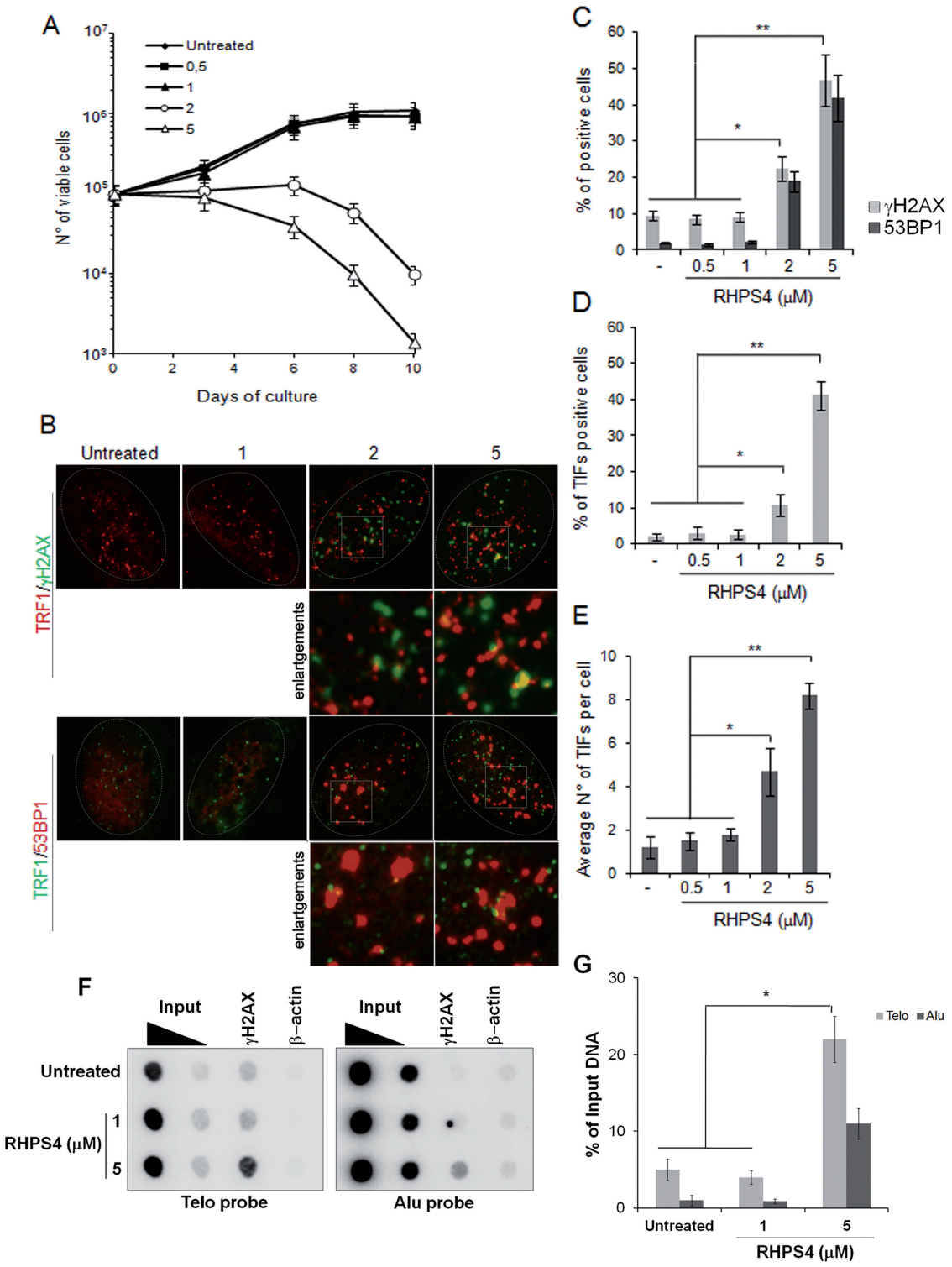

Figure 2. RHPS4 displays a narrow window for selectivity between normal and tumor cells. BJ-hTERT cells were treated with rising concentration of RHPS4 as indicated. Curves in (**A**) report the number of viable cells at each time point in untreated or chronically treated cells. (**B**) BJ-hTERT fibroblasts were treated with the indicated concentration of RHPS4 for 24 h, fixed and processed for co-IF against γH2AX/TRF1 or 53BP1/TRF1. Representative images of colocalizations are shown (Leica deconvolution microscope 100× magnification). Histograms in (**C**) report the percentage of γH2AX (bright gray bars) and 53BP1 (dark gray bars) foci positive cells. TIFs positive cells, scored as the percentage of cells displaying more than 4 γH2AX/TRF1 colocalizations, are shown in (**D**) and the average number of TIFs is reported in (**E**). The mean of three independent experiments with comparable results is shown. (**F**) ChIP experiments performed on BJ-hTERT untreated or exposed for 24 h to doses 1 and 5 μM of RHPS4. Immuno-precipitations were performed with antibodies against γH2AX and β-actin as negative control. The total DNA (input) represents 10% and 1% of genomic DNA. The precipitated DNA was analyzed by dot blot with telomeric and Alu probes. (**G**) The densitometric evaluation is reported in the histogram as percent of precipitated DNA versus telomeric (Telo) or genomic DNA (Alu). Error bars indicate SD. $*P < 0.05$, $**P < 0.01$.

of phospho-H2AX and 53BP1 foci (Figure 3A, B and D) and at telomeres, as revealed by the number of TIF (corresponding to a colocalization of phospho-H2AX foci with telomeres) (Figure 3D–F and Supplementary Figure S6) and by the ratio between telomeric and non-telomeric DNA damage evaluated in ChIP experiments (Figure 3G and H). Consistent with interphase data, TIFs in metaphase (meta-TIF), which allow to accurately estimate the TIFs number in a whole nucleus (34) and avoid including TIFs postulated to transiently occur during the S/G2 phases (39), were detected in BJ-EHLT but not in BJ cells (Figure 4A and B). Interestingly, the levels of telomeric and non-telomeric DNA damage induced by RHPS4, as revealed by IF and ChIP assay, strongly correlated with the susceptibility to the drug (Figures 3 and 4A and B).

Meta-TIFs occurred independently of the telomere length status (Figure 4C) and were observed preferentially on chromatids with normal telomere signals (Figure 4D). These results, together with the lack of 53BP1 recruitment in untreated BJ-EHLT cells (Figure 3B and D) and with the fact that these cells did not exhibit a significant increase of end-to-end fusions (Figure 3C) and telomere rearrangements (Figure 4E), suggest that telomeres of RHPS4 sensitive cells are only partially uncapped. It is worth noting that a significant number of aberrant telomere signals was also induced by the Ras/V12 expression, probably due to the replicative stress caused by the oncogene, which was further increased by G4 ligand treatment (Figure 3C and 4E).

The fact that transformed and tumor cells exhibit a higher level of basal telomere uncapping than normal cells and are more prone to damage following G4 stabilization was confirmed in spontaneously transformed human fibroblasts and in normal versus transformed cells of different hystological origin (Figure 3 and Supplementary Figure S7).

Artificially created telomere deprotection sensitizes normal cells to G-quadruplex stabilization

One of the mechanisms of the accumulation of partially uncapped telomeres in transformed cells, without any overt consequences on cell growth, could be the failure in cell-cycle checkpoint pathways. Thus, we generated p53 and pRb-compromised BJ-hTERT cell lines and evaluated the effects of RHPS4 treatment in terms of cell viability and activation of DDR pathway. In control (shGFP) as well as in pRb-compromised cells (Figure 5A), we did not observe a substantial activation of DDR at telomeres (Figure 5B–E) and treatment with the G4 ligand RHPS4 neither affected cell viability (Figure 5F) nor induced DNA damage, both at telomeric and non-telomeric regions (Figure 5B–E). In contrast, knock-down of p53 (Figure 5A), by itself, was enough able to induce H2AX phosphorylation both globally and at telomeres (Figure 5B–E), without activation of a complete DDR cascade, as shown by the lack of the phosphorylated form of Chk2 (Figure 5B). Exposure of p53-compromised cells to RHPS4 markedly increased telomere uncapping and growth defects (Figure 5C–F). In agreement with the increased dosage of TRF2 in BJ-EHLT, as compared to BJ or BJ-hTERT cells (40), and with the data showing that p53 controls TRF2 stability (41), p53-compromised BJ-hTERT cells expressed high levels of TRF2 (Figure 5G), which could allow these cells to tolerate the accumulation of deprotected telomeres.

Results described up to now suggest that the effects of G4 ligands on transformed and tumor cells could result from the presence of a basal degree of telomere deprotection. The functional relevance of this observation was directly assessed by experimentally generating telomere deprotection through RNA interference against the shelterin protein TRF2. Interestingly, cells partially depleted of TRF2 (Figure 6A) showed a telomere-driven DDR, as revealed by co-IF and ChIP experiments (Figure 6 A–D), and were prone to RHPS4-induced telomere damage (Figure 6A–D) and cell growth inhibition (Figure 6E). Therefore, a partial telomere uncapping is sufficient to render cells sensitive to RHPS4.

DISCUSSION

Evidence showing that telomeric G4 ligands selectively impair the growth of cancer cells without affecting the viability of normal cells (mainly fibroblasts) points to these molecules as possible drug candidate for future clinical applications (19).

Here, we report that the sensitivity of G4 ligands toward transformed cells is not restricted to fibroblasts but it is a general phenomenon observed in several lines from normal and tumor counterpart of different hystotype. Moreover, normal cells are not completely resistant to telomere damage induced by G4 stabilization, but a 4-fold higher dosage of compound is necessary to induce telomere damage and anti-proliferative defects in normal cells. These results, together with the comparable drug uptake between normal and transformed cells, clearly exclude the possibility that G4 ligands are unable to target telomeres in normal cells. Moreover, the high susceptibility of transformed cells to G4 stabilization was not associated to telomere length nor to their high replication rate. Therefore, due to the lack of any activation of DDR in normal cells at the drug dose able to significantly damage telomeres of transformed cells, we can assert that telomeres of transformed cells are more prone to be damaged by G4 ligands. In this regard we can rule out the effect of the RHPS4 on the G4 structure recently identified within the 5′UTR of TRF2 mRNA (42), since no change in the expression of this telomeric protein was observed upon treatment (37); even if the effects of the drug on other G4 structures throughout the genome (43,44) may contribute to increase the therapeutic index of this new class of potential antitumoral agents.

In this work, we studied the mechanisms underlying the differential response to G4 ligand between normal and tumor cells. Although an increased level of DDR markers thorughout the genome was observed in transformed compared to normal cells, we found a striking correlation between a basal degree of telomere damage and an enhanced sensitivity to RHPS4 in transformed cells. This occurred independently on telomere length and was characterized by an activation of γH2AX at telomeres without 53BP1 recruitment and telomere rearrangements. These data are in agreement with evidence showing that some cancer and immortalized human cell lines carry an excessive burden

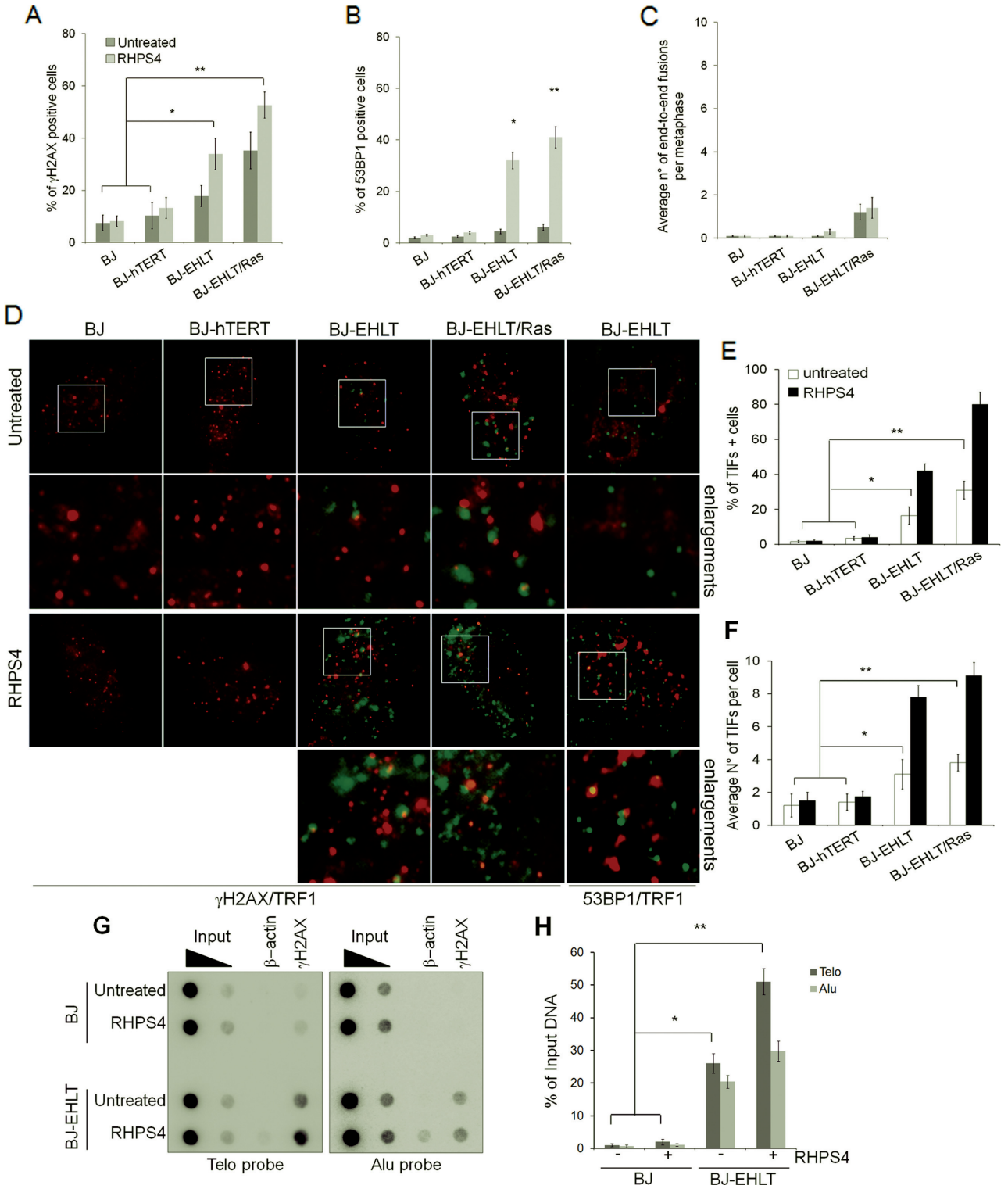

Figure 3. An excessive burden of DDR characterizes telomeres of transformed cells. The indicated cell populations were treated with 0.5 μM RHPS4 for 24 h, fixed, processed for co-IF analysis against γH2AX/TRF1 and 53BP1/TRF1 and finally scored for the percentage of γH2AX (**A**) or 53BP1 (**B**) foci-positive cells. (**C**) Cells treated as above were blocked in metaphase and processed for the cytogenetic analysis of end-to-end fusions. Histograms represent the average number of end-to-end fused chromosomes per metaphase. (**D**) Representative images of co-localizations between TRF1 (red) and γH2AX (green) or TRF1 (green) and 53BP1 (red) are shown (Leica Deconvolution microscope 100× magnification). The percentage of TIFs-positive cells (calculated as cells displaying more than 4 TRF1/ γH2AX co-localizations) is shown in (**E**) and the average number of TIFs per nucleus of untreated and treated samples in (**F**). The mean of three independent experiments with similar results is reported. (**G**) ChIP experiments performed on BJ and BJ-EHLT untreated or exposed for 24 h to 0.5 μM RHPS4. Immuno-precipitations were performed with antibodies against γH2AX and β-actin as negative control. The precipitated DNA was analyzed by dot blot with telomeric and Alu probes. (**H**) The densitometric evaluation is reported in the histograms as percent of precipitated DNA versus telomeric (Telo) or genomic DNA (Alu). Error bars indicate SD. $^{*}P < 0.05$, $^{**}P < 0.01$.

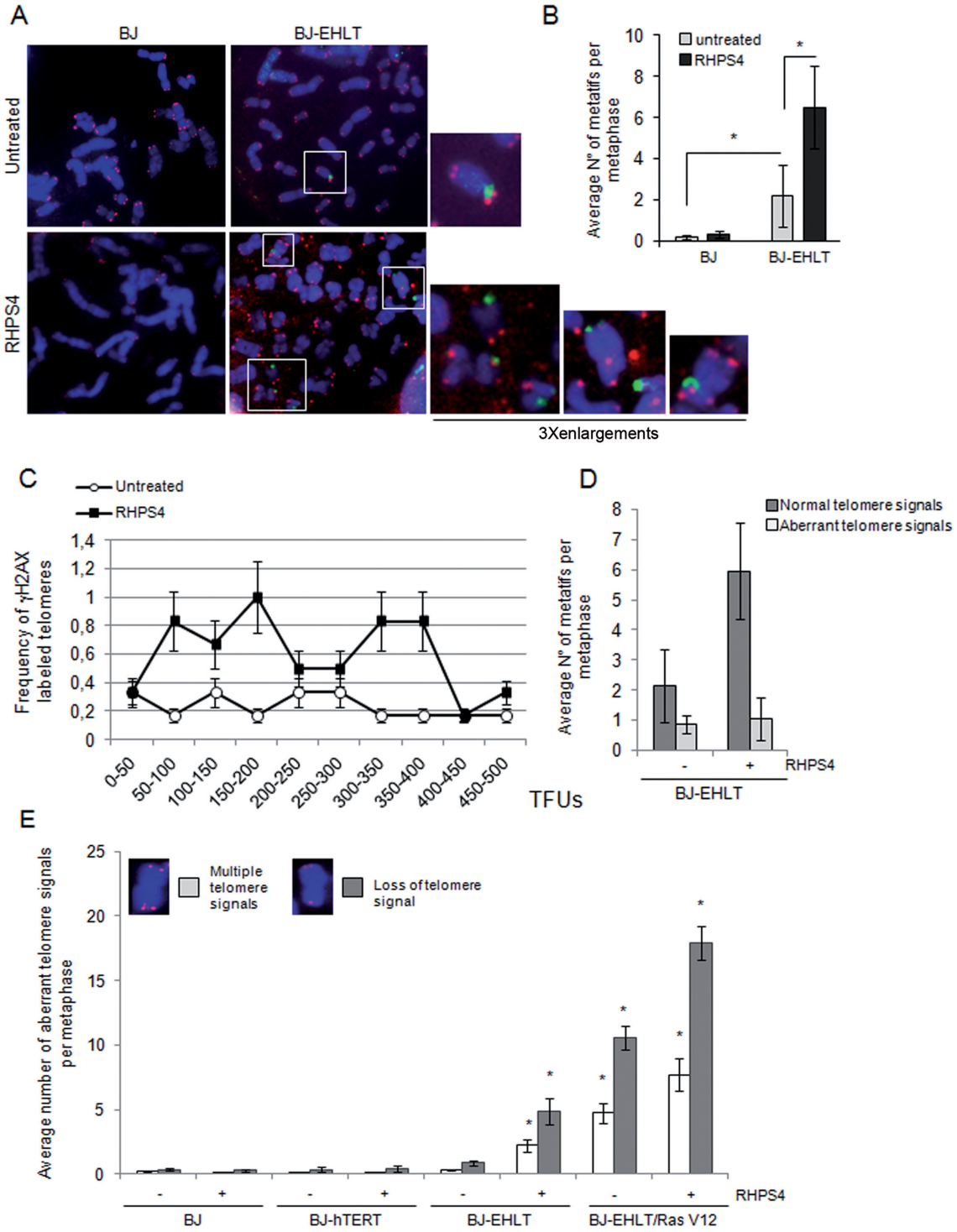

Figure 4. DDR markers at telomeres in transformed cells are associated with RHPS4 sensitivity. Normal (BJ) and transformed fibroblasts (BJ-EHLT) were treated with 0.5 μM RHPS4 for 24 h, processed for meta-TIFs analysis with the γH2AX antibody (green) and Telo PNA probe (red) and then counterstained with DAPI (blue). Representative images at 100× magnification are shown in (**A**) and 3× enlargements are shown. Histograms in (**B**) report the average number of γH2AX labeled telomere per metaphase (meta-TIFs) calculated on 20 metaphases per sample in each experiment. (**C**) BJ-EHLT treated as above were processed for qFISH analysis for the quantification of telomere signal intensities (expressed as telomere fluorescence units) and the frequence of γH2AX labeled telomeres in each category of signal intensity is reported in the curves in untreated and treated conditions. The average number of meta-TIFs associated with a normal (a single telomeric spot per chromatid) or an aberrant (absent or multiple telomeric spots, decrease of telomere spot intensities) telomere signal is shown in (**D**). The indicated cell lines untreated or treated as above described, were processed for FISH staining with a Telo PNA probe (red) and counterstained by DAPI and then scored for the quantification of telomere aberration. (**E**) Histograms report the average number of aberrant telomere signals per metaphase in the indicated categories, calculated on 20 metaphases per sample in each experiment. Representative images of the telomere aberrations are reported inside the histogram. The mean of three independent experiments with comparable results is shown. Error bars indicate SD. $^*P < 0.05$.

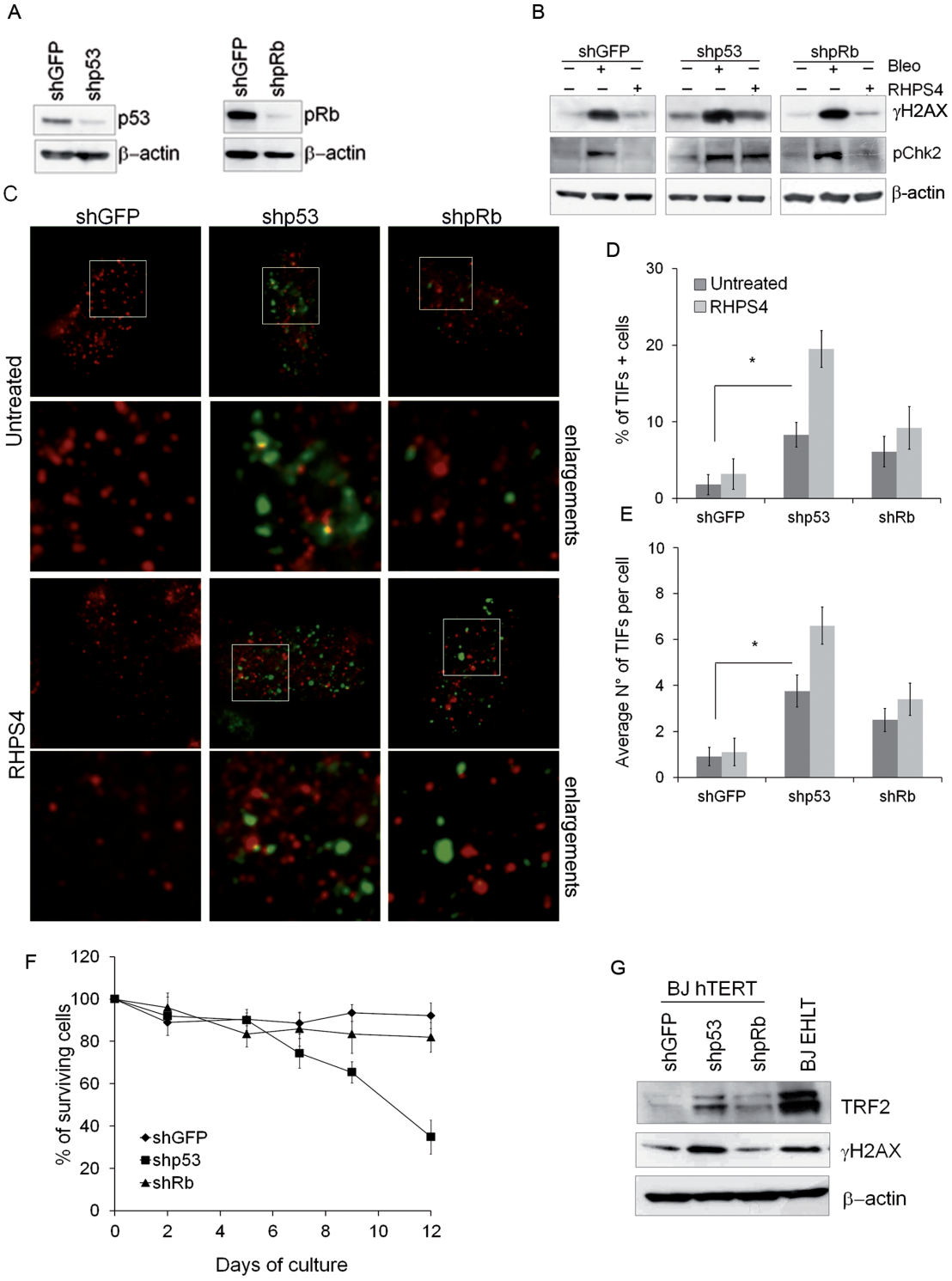

Figure 5. Abrogation of p53 pathway triggers DDR at telomeres and sensitizes cells to RHPS4. (**A**) Western blot analysis of p53 and pRb expression in BJ-hTERT stably infected with a retrovirus carrying a control short hairpin (shGFP), and shp53 or shpRb, respectively. (**B**) Western blot analysis of DDR proteins in GFP, p53 or pRb interfered BJ-hTERT cells untreated and treated with 30 μM Bleomycin (Bleo, Sigma) for 30 min or 0.5 μM RHPS4 for 96 h. β-actin is shown as loading control. (**C**) Representative images of IF analysis of DNA damage activation in BJ-hTERT cell lines upon 24 h exposure of 0.5 μM RHPS4: co-IF against γH2AX and TRF1 was performed and images captured with a Leica Deconvolution microscope (magnification 100×). (**D**) Percentage of the TIFs-positive cells and of the average number of TIFs per nucleus (**E**) in treated and control samples. The mean of three independent experiments with similar results is reported. **(F)** shGFP-, p53- or pRb-interfered BJ-hTERT cells were treated with 0.5 μM RHPS4 and at the indicated times cells were counted and the viability determined. The graph reports the percentage of surviving cells in treated versus untreated samples. The mean of three independent experiments with comparable results is shown. (**G**) Western blot analysis of TRF2 and γH2AX levels in the indicated cell lines. The levels of β-actin were provided as loading control. Results showed are representative of three independent experiments with comparable results. Error bars indicate SD. $*P < 0.05$.

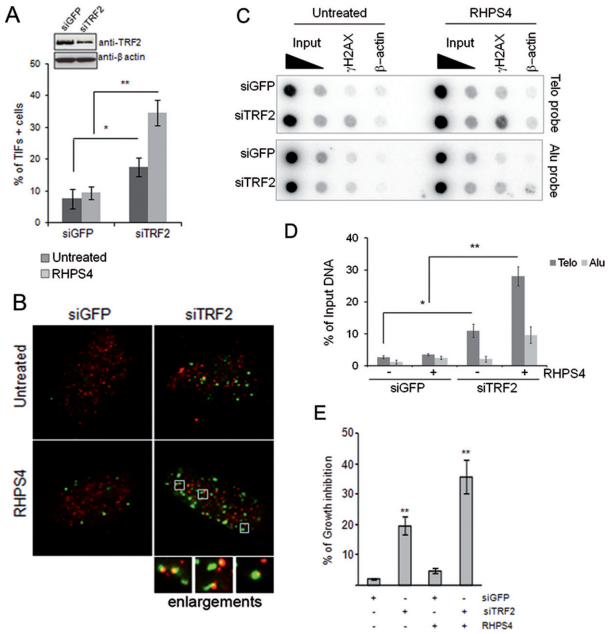

Figure 6. Telomere deprotection sensitizes normal cells to RHPS4. (**A**) BJ-hTERT fibroblasts were transfected with siRNA against GFP and the shelterin protein TRF2. Transfected cells were treated with 0.5 μM RHPS4 for 24 h or left untreated. At the end of treatment cells were processed for co-IF against γH2AX (green) and TRF1 (red) and the percentage of TIFs positive cells in each sample was scored and reported in the histograms. Representative images of TIFs at 100× magnification are shown in (**B**). (**C**) siGFP and siTRF2 transfected BJ-hTERT cells were exposed for 24 h with 0.5 μM RHPS4 and processed for ChIP with antibodies against γH2AX and β-actin as negative control. The precipitated DNA was analyzed by dot blot with telomeric and Alu probes. (**D**) The densitometric evaluation is reported in the histogram as percent of precipitated DNA versus telomeric (Telo) or genomic DNA (Alu). (**E**) Cells transfected as above and treated for 72 h with 0.5 μM RHPS4 were counted and viability determined by tripan blue exclusion. Histograms report the percentage of growth inhibition compared to untransfected untreated samples. Error bars indicate SD. $*P < 0.05$, $**P < 0.01$.

of DDR+ telomeres (19) that is independent of telomere length (here and (8,45–46)). Furthermore, we provided a causal nexus between telomere uncapping, artificially induced by TRF2 depletion and cell sensitivity to RHPS4 treatment in normal cells. Nevertheless, we cannot exclude that extra-telomeric loci, targeted by G4 ligands, may contribute to confer sensitivity to transformed cells. In seemingly apparent contradiction with this result, transformed and cancer cells used in this study showed an increased level of TRF2, in agreement with the enhanced stability of TRF2 previously observed in p53-deficient cells (41). This suggests that the cause of the increased rate of telomere uncapping in cancer and transformed BJ cells we used here, is not the TRF2 depletion. Since a reduced expression of p53 in normal cells is sufficient to increase the basal level of uncapped telomeres and RHPS4 sensitivity, p53 could control the tolerance toward partial telomere uncapping or affect telomere structure or both. We propose that transformation triggers replication stress and partially uncapped telomeres, which are prone to induce a detrimental DDR response upon G4 ligand treatment. However, how the presence of telomere-associated DDR in transformed cells makes them susceptible to telomeric G4 stabilization remains to be determined. In this context, while it could be easy to hypothesize that in agreement with the induction of replicative senescence (15), a threshold number of TIFs can be quickly reached in transformed cells (already possessing DDR+ telomeres) when exposed to G4 ligands, the lack of any DDR+ telomeres in drug-treated normal telomerized cells excludes this hypothesis. One can hazard the guess that the increased telomere uncapping triggered by G4 ligands might further increase genomic instability, such as cancer cells die of crisis by 'tipping the balance' (47).

In conclusion, this work adds a piece of substantial evidence accounting for the presence of uncapped telomeres in transformed cells, and for their role as determinants of susceptibility to G4 stabilizing molecules.

SUPPLEMENTARY DATA

Supplementary Data are available at NAR Online.

FUNDING

Italian Association for Cancer Research (A.I.R.C., # 11567 to A.B. and # 14337 to C.L.]; la Ligue contre la cancer [to E.G. equipe labelisée]; INCa program TELOCHROM [to E.G.]. Italian Foundation for Cancer Research (F.I.R.C.) [to C.C.]. Umberto Veronesi Foundation [to E.S. and A.R.]. Funding for open access charge: Italian Association for Cancer Research [A.I.R.C., # 11567 to A.B. and # 14337 to C.L.].
Conflict of interest statement. None declared.

REFERENCES

1. Griffith,J.K., Bryant,J.E., Fordyce,C.A., Gilliland,F.D., Joste,N.E. and Moyzis,R.K. (1999) Reduced telomere DNA content is correlated with genomic instability and metastasis in invasive human breast carcinoma. *Breast Cancer Res. Treat.*, **54**, 59–64.
2. Oganesian,L. and Bryan,T.M. (2007) Physiological relevance of telomeric G-quadruplex formation: a potential drug target. *BioEssays*, **29**, 155–165.
3. de Lange,T. (2005) Shelterin: the protein complex that shapes and safeguards human telomeres. *Genes Dev.*, **19**, 2100–2110.
4. Palm,W. and de Lange,T. (2008) How shelterin protects mammalian telomeres. *Ann. Rev. Genet.*, **42**, 301–334.
5. de Lange,T. (2010) How shelterin solves the telomere end-protection problem. *Cold Spring Harb. Symp. Quant. Biol.*, **75**, 167–177.
6. Verdun,R.E. and Karlseder,J. (2006) The DNA damage machinery and homologous recombination pathway act consecutively to protect human telomeres. *Cell*, **127**, 709–720.
7. O'Sullivan,R.J. and Karlseder,J. (2010) Telomeres: protecting chromosomes against genome instability. *Nat. Rev.*, **11**, 171–181.
8. Smogorzewska,A., Karlseder,J., Holtgreve-Grez,H., Jauch,A. and de Lange,T. (2002) DNA ligase IV-dependent NHEJ of deprotected mammalian telomeres in G1 and G2. *Curr. Biol.*, **12**, 1635–1644.
9. Rai,R., Zheng,H., He,H., Luo,Y., Multani,A., Carpenter,P.B. and Chang,S. (2010) The function of classical and alternative non-homologous end-joining pathways in the fusion of dysfunctional telomeres. *EMBO J.*, **29**, 2598–2610.
10. Takai,H., Smogorzewska,A. and de Lange,T. (2003) DNA damage foci at dysfunctional telomeres. *Curr. Biol.*, **13**, 1549–1556.
11. Hockemeyer,D., Daniels,J.P., Takai,H. and de Lange,T. (2006) Recent expansion of the telomeric complex in rodents: Two distinct POT1 proteins protect mouse telomeres. *Cell*, **126**, 63–77.
12. Denchi,E.L. and de Lange,T. (2007) Protection of telomeres through independent control of ATM and ATR by TRF2 and POT1. *Nature*, **448**, 1068–1071.

13. d'Adda di Fagagna,F., Reaper,P.M., Clay-Farrace,L., Fiegler,H., Carr,P., Von Zglinicki,T., Saretzki,G., Carter,N.P. and Jackson,S.P. (2003) A DNA damage checkpoint response in telomere-initiated senescence. *Nature*, **426**, 194–198.
14. Cesare,A.J. and Karlseder,J. (2012) A three-state model of telomere control over human proliferative boundaries. *Curr. Opin. Cell Biol.*, **24**, 731–738.
15. Kaul,Z., Cesare,A.J., Huschtscha,L.I., Neumann,A.A. and Reddel,R.R. (2012) Five dysfunctional telomeres predict onset of senescence in human cells. *EMBO Rep.*, **13**, 52–59.
16. Fumagalli,M., Rossiello,F., Clerici,M., Barozzi,S., Cittaro,D., Kaplunov,J.M., Bucci,G., Dobreva,M., Matti,V., Beausejour,C.M. *et al.* (2012) Telomeric DNA damage is irreparable and causes persistent DNA-damage-response activation. *Nat. Cell Biol.*, **14**, 355–365.
17. Kelland,L. (2007) Targeting the limitless replicative potential of cancer: the telomerase/telomere pathway. *Clin. Cancer Res.*, **13**, 4960–4963.
18. Neidle,S. (2010) Human telomeric G-quadruplex: the current status of telomeric G-quadruplexes as therapeutic targets in human cancer. *FEBS J.*, **277**, 1118–1125.
19. Bidzinska,J., Cimino-Reale,G., Zaffaroni,N. and Folini,M. (2013) G-quadruplex structures in the human genome as novel therapeutic targets. *Molecules*, **18**, 12368–12395.
20. Lavrado,J., Moreira,R. and Paulo,A. (2010) Indoloquinolines as scaffolds for drug discovery. *Curr. Med. Chem.*, **17**, 2348–2370.
21. Casagrande,V., Salvati,E., Alvino,A., Bianco,A., Ciammaichella,A., D'Angelo,C., Ginnari-Satriani,L., Serrilli,A.M., Iachettini,S., Leonetti,C. *et al.* (2011) N-cyclic bay-substituted perylene G-quadruplex ligands have selective antiproliferative effects on cancer cells and induce telomere damage. *J. Med. Chem.*, **54**, 1140–1156.
22. Riou,J.F. (2004) G-quadruplex interacting agents targeting the telomeric G-overhang are more than simple telomerase inhibitors. *Curr. Med. Chem.*, **4**, 439–443.
23. Leonetti,C., Amodei,S., D'Angelo,C., Rizzo,A., Benassi,B., Antonelli,A., Elli,R., Stevens,M.F., D'Incalci,M., Zupi,G. *et al.* (2004) Biological activity of the G-quadruplex ligand RHPS4 (3,11-difluoro-6,8,13-trimethyl-8H-quino[4,3,2-kl]acridinium methosulfate) is associated with telomere capping alteration. *Mol. Pharmacol.*, **66**, 1138–1146.
24. Counter,C.M., Meyerson,M., Eaton,E.N., Ellisen,L.W., Caddle,S.D., Haber,D.A. and Weinberg,R.A. (1998) Telomerase activity is restored in human cells by ectopic expression of hTERT (hEST2), the catalytic subunit of telomerase. *Oncogene*, **16**, 1217–1222.
25. Zongaro,S., de Stanchina,E., Colombo,T., D'Incalci,M., Giulotto,E. and Mondello,C. (2005) Stepwise neoplastic transformation of a telomerase immortalized fibroblast cell line. *Cancer Res.*, **65**, 11411–11418.
26. Marra,M., Salzano,G., Leonetti,C., Porru,M., Franco,R., Zappavigna,S., Liguori,G., Botti,G., Chieffi,P., Lamberti,M. *et al.* (2012) New self-assembly nanoparticles and stealth liposomes for the delivery of zoledronic acid: a comparative study. *Biotechnol. Adv.*, **30**, 302–309.
27. Salvati,E., Leonetti,C., Rizzo,A., Scarsella,M., Mottolese,M., Galati,R., Sperduti,I., Stevens,M.F., D'Incalci,M., Blasco,M. *et al.* (2007) Telomere damage induced by the G-quadruplex ligand RHPS4 has an antitumor effect. *J. Clin. Investig.*, **117**, 3236–3247.
28. Castro-Vega,L.J., Jouravleva,K., Liu,W.Y., Martinez,C., Gestraud,P., Hupe,P., Servant,N., Albaud,B., Gentien,D., Gad,S. *et al.* (2013) Telomere crisis in kidney epithelial cells promotes the acquisition of a microRNA signature retrieved in aggressive renal cell carcinomas. *Carcinogenesis*, **34**, 1173–1180.
29. Grandori,C., Wu,K.J., Fernandez,P., Ngouenet,C., Grim,J., Clurman,B.E., Moser,M.J., Oshima,J., Russell,D.W., Swisshelm,K. *et al.* (2003) Werner syndrome protein limits MYC-induced cellular senescence. *Genes Dev.*, **17**, 1569–1574.
30. Boehm,J.S., Hession,M.T., Bulmer,S.E. and Hahn,W.C. (2005) Transformation of human and murine fibroblasts without viral oncoproteins. *Mol. Cell. Biol.*, **25**, 6464–6474.
31. Heald,R.A., Modi,C., Cookson,J.C., Hutchinson,I., Laughton,C.A., Gowan,S.M., Kelland,L.R. and Stevens,M.F. (2002) Antitumor polycyclic acridines. 8.(1) Synthesis and telomerase-inhibitory activity of methylated pentacyclic acridinium salts. *J. Med. Chem.*, **45**, 590–597.
32. Biroccio,A., Porru,M., Rizzo,A., Salvati,E., D'Angelo,C., Orlandi,A., Passeri,D., Franceschin,M., Stevens,M.F., Gilson,E. *et al.* (2011) DNA damage persistence as determinant of tumor sensitivity to the combination of Topo I inhibitors and telomere-targeting agents. *Clin. Cancer Res.*, **17**, 2227–2236.
33. Biroccio,A., Benassi,B., Filomeni,G., Amodei,S., Marchini,S., Chiorino,G., Rotilio,G., Zupi,G. and Ciriolo,M.R. (2002) Glutathione influences c-Myc-induced apoptosis in M14 human melanoma cells. *J. Biol. Chem.*, **277**, 43763–43770.
34. Cesare,A.J., Kaul,Z., Cohen,S.B., Napier,C.E., Pickett,H.A., Neumann,A.A. and Reddel,R.R. (2009) Spontaneous occurrence of telomeric DNA damage response in the absence of chromosome fusions. *Nat. Struct. Mol. Biol.*, **16**, 1244–1251.
35. Lenain,C., Bauwens,S., Amiard,S., Brunori,M., Giraud-Panis,M.J. and Gilson,E. (2006) The Apollo 5′ exonuclease functions together with TRF2 to protect telomeres from DNA repair. *Curr. Biol.*, **16**, 1303–1310.
36. Salvati,E., Scarsella,M., Porru,M., Rizzo,A., Iachettini,S., Tentori,L., Graziani,G., D'Incalci,M., Stevens,M.F., Orlandi,A. *et al.* (2010) PARP1 is activated at telomeres upon G4 stabilization: possible target for telomere-based therapy. *Oncogene*, **29**, 6280–6293.
37. Rizzo,A., Salvati,E., Porru,M., D'Angelo,C., Stevens,M.F., D'Incalci,M., Leonetti,C., Gilson,E., Zupi,G. and Biroccio,A. (2009) Stabilization of quadruplex DNA perturbs telomere replication leading to the activation of an ATR-dependent ATM signaling pathway. *Nucleic Acids Res.*, **37**, 5353–5364.
38. Belgiovine,C., Frapolli,R., Bonezzi,K., Chiodi,I., Favero,F., Mello-Grand,M., Dei Tos,A.P., Giulotto,E., Taraboletti,G., D'Incalci,M. *et al.* (2010) Reduced expression of the ROCK inhibitor Rnd3 is associated with increased invasiveness and metastatic potential in mesenchymal tumor cells. *PloS ONE*, **5**, e14154.
39. Verdun,R.E., Crabbe,L., Haggblom,C. and Karlseder,J. (2005) Functional human telomeres are recognized as DNA damage in G2 of the cell cycle. *Mol. Cell*, **20**, 551–561.
40. Biroccio,A., Cherfils-Vicini,J., Augereau,A., Pinte,S., Bauwens,S., Ye,J., Simonet,T., Horard,B., Jamet,K., Cervera,L. *et al.* (2013) TRF2 inhibits a cell-extrinsic pathway through which natural killer cells eliminate cancer cells. *Nat. Cell Biol.*, **15**, 818–828.
41. Fujita,K., Horikawa,I., Mondal,A.M., Jenkins,L.M., Appella,E., Vojtesek,B., Bourdon,J.C., Lane,D.P. and Harris,C.C. (2010) Positive feedback between p53 and TRF2 during telomere-damage signalling and cellular senescence. *Nat. Cell Biol.*, **12**, 1205–1212.
42. Gomez,D., Guedin,A., Mergny,J.L., Salles,B., Riou,J.F., Teulade-Fichou,M.P. and Calsou,P. (2010) A G-quadruplex structure within the 5′-UTR of TRF2 mRNA represses translation in human cells. *Nucleic Acids Res.*, **38**, 7187–7198.
43. Salvati,E., Zizza,P., Rizzo,A., Iachettini,S., Cingolani,C., D'Angelo,C., Porru,M., Randazzo,A., Pagano,B., Novellino,E. *et al.* (2014) Evidence for G-quadruplex in the promoter of vegfr-2 and its targeting to inhibit tumor angiogenesis. *Nucleic Acids Res.*, **42**, 2945–2957.
44. Biffi,G., Tannahill,D., McCafferty,J. and Balasubramanian,S. (2013) Quantitative visualization of DNA G-quadruplex structures in human cells. *Nat. Chem.*, **5**, 182–186.
45. Augereau,A., T'Kint de Roodenbeke,C., Simonet,T., Bauwens,S., Horard,B., Callanan,M., Leroux,D., Jallades,L., Salles,G., Gilson,E. *et al.* (2011) Telomeric damage in early stage of chronic lymphocytic leukemia correlates with shelterin dysregulation. *Blood*, **118**, 1316–1322.
46. Cesare,A.J., Hayashi,M.T., Crabbe,L. and Karlseder,J. (2013) The telomere deprotection response is functionally distinct from the genomic DNA damage response. *Mol. Cell*, **51**, 141–155.
47. Jacobs,J.J. (2013) Loss of telomere protection: consequences and opportunities. *Front. Oncol.*, **3**, doi:10.3389/fonc.2013.00088.